ISSN 1392-1207. MECHANIKA. Vol. 30, No. 6, 2024: 514–522

Dynamic Modelling and Analysis of a New Design Variable Inertia Flywheel for Diesel Engine Using Bond Graph Technique

Prabhat R. MAHTO*, Anil C. MAHATO**
**Department of Mechanical Engineering, Birla Institute of Technology, Mesra, Ranchi, Jharkhand-835215, India, E-mail: prabhat.mahto@bitmesra.ac.in*
***Department of Mechanical Engineering, Birla Institute of Technology, Mesra, Ranchi, Jharkhand-835215, India, E-mail: anilmahato@bitmesra.ac.in*
https://doi.org/10.5755/j02.mech.35855

1. Introduction

A mechanical device used to reduce the speed fluctuations and input/output energy variations of rotating machinery when sudden load variation is engaged is known as a flywheel. It may also be used as an energy storage device. The conventional flywheel is simple in working principle, has high inertia, and is bulky. It does not support the engine for easy start-up due to high torque requirements. However, its applications may include an internal combustion engine, industrial machinery like camshafts, alternating current generators etc. Besides energy storage applications, it may be used in flywheel-based hybrid vehicles, uninterrupted power supplies, cyclic alternative energy sources such as wind turbines, wave energy, and space power systems [1]. Therefore, a flywheel capable of varying the inertia using various techniques is highly desirable to reduce the start-up torque of the machine [2]. The mathematical equation of the conventional constant inertial-based flywheel is very simple, and its energy storage capability depends on the angular speed and the moment of inertia of the flywheel. In a conventional flywheel, the moment of inertia is fixed. Hence, the energy storage capability is varied only with the variation of the angular speed of the flywheel. Besides, in a variable inertia flywheel, the same objective can be satisfied effectively by changing both moment of inertia as well as the angular speed of the flywheel. Therefore, an additional adjustable parameter i.e. moment of inertia of the flywheel, makes it more flexible for variable loading systems. Also, the variable inertia flywheel is smaller, lighter, and has better control effects. It may eliminate the need for a continuously variable transmission between the flywheel and the load [3]. This is primarily used in spacecraft adaptive attitude control and kinematic energy storage and is hardly used to reduce the speed fluctuations of the rotating machinery [4]. Recently, an overview of various designs of the variable inertia flywheel was discussed by Kumar *et al.* [5]. Previously, multiple researchers proposed multiple ways to vary the inertia of the flywheel, such as by adding fluid to the flywheel [6-12], allowing the flywheel material to strain [13], moving mechanical masses [14-18] etc. In [6], Van de Ven introduces a concept of fluidic variable inertia flywheel that allows the liquid to fill into it is moved freely between a central port in the flywheel and the tank, which is at atmospheric pressure. Moreover, in [7-8], authors use a similar concept to control the inertia in wind turbines. However, these flywheels have some drawbacks. It develops stress at its wall due to the fluid pressure and the swirl of the fluid. Limited literatures are available on the fluid-based variable inertia flywheel concept. However, several patients are awarded for the similar concepts [9-11]. Another concept for variable inertia flywheel is based on an elastomer ring which expanses in a non-linear way. The elastic and centrifugal force together deliver remarkable energy extraction (about 80%) at almost constant angular speed [12]. The limitation of elastomeric materials along with the necessary stress-strain properties, this model significantly restricts the energy density of the flywheel. Furthermore, in the third concept, to obtain variable moment inertia from the flywheel, the mechanical mass elements are moved radially outward direction due to the centrifugal force exerted on it. These mass elements are then retracted using springs or gravity. Previously, several researchers used the stated principle to obtain variable inertia [13-17]. In [13], a two-terminal mass concept, together with an electro-hydraulic approach, is used to obtain a variable equivalent mass. The technology to obtain an equivalent inertial mass between two terminals of the component is analyzed dynamically, and further, a prototype is tested on a test bed. The application of the two terminals mass concept is extended in the vehicle suspension system to absorb the vibration [14]. The adjustable moment of inertia is achieved from the embedded flywheel by the movement of the sliders or masses toward the radially outward direction. The dynamical performance of the stated concept has been analyzed by simulation, and validated experimentally. In addition, different vehicle suspension parameters like road handling and safety, ride comfort, suspension deflection etc. are compared with the responses whenever a constant inertia-based flywheel is incorporated into the system. It has been observed that the system with a two-terminal mass-based variable inertia flywheel provides better results [14]. Yang *et al*. propose a similar scheme where the detailed design of the two-terminal mass device with variable inertia flywheel has been discussed [15]. In [16], Ning *et al*. proposed a rotary variable admittance which is composed of two variable inertia flywheel and MRF damper. It is incorporated into the seat suspension to control the vibration of the automotive seating system. In [17-18], the rotational inertial of the flywheel is estimated in a diesel generator for pulse load conditions. These studies concluded that the variable inertia flywheel could stabilize the diesel generator speed. Zhang *et al*. present another similar work in [19], where a novel design of variable inertia flywheel is presented for application on diesel generators. The impact of sudden loading and unloading on the stated engine is analyzed in the presence of the proposed variable inertia flywheel. In [20], Mahato et al. stud-

ied variable inertia flywheels regarding the potential for energy saving in power hydraulic systems. It reduces the passive vibration in the power hydraulic system and decreases the pressure surge. Therefore, authors have analyzed whether variable inertia flywheels have any role in energy saving or not. The simulation results confirm that the variable inertia flywheel does not take part in energy saving in the system. Another work on a hydraulic motor drive with variable inertia flywheel is presented by Kushwaha *et al*. in [21]. In this study, authors analyzed the dynamic performance of the hydraulic drive system in the presence of variable inertia flywheel and fixed inertia flywheel separately. Also, recently, the application of the variable inertia flywheel has been extended to wave energy converters [22] and flywheel-based energy storage systems [23]. In [22], the dynamics of variable inertia flywheel is established numerically and validated it's adaptively by changing wave conditions, whereas in [23], the fixed inertia flywheel is replaced by a variable inertia flywheel to store the energy in a fixed speed flywheel energy storage system. The literatures i.e. [13-23] are based on a similar design of variable inertia flywheel, which is mainly composed of several components like four sliders, four compression springs, outer ring, inside housing etc. The higher number of mechanical mass elements makes the system dynamics more complex.

To reduce the complexity of the dynamical system modeling, a novel design of a variable inertia flywheel is proposed. In the proposed design, the variable inertia flywheel is composed of only two sliders, four springs, four supporting rods, and a metal ring. A dynamic model of a diesel engine with a variable inertia flywheel is developed and simulated using the Bond graph technique. Bond graph is a tool used to represent the physical dynamical system. This is capable of converting the system into state-space form and also interacting with the multi-energy domains [24-25]. The diesel engine with VI_F is simulated using SYMBOLS SHAKTI software [26], analyzed the effect of the key parameters on the system performance.

2. Proposed Model of the Diesel Engine with Variable Inertia Flywheel (VI_F)

The schematic diagram of the diesel engine with the proposed VI_F is shown in Fig. 1. From Fig. 1, the VI_F is installed on the shaft of the diesel engine. The VI_F is an assembly of the outer metal ring, four supporting rods, two cover plates, two slider-supported rods, two sliders, a shaft holding the inner metal ring, and four helical springs. The rotating shaft of the diesel engine and the VI_F are fitted by a key element. The hollow sliders are mounted on the slider-supported rods and travel along the length of the supporting rods, and each slider is connected with two compression springs. The other end of the springs is connected with an outer metal ring of the VI_F (Fig. 1). Whenever the speed of the rotating shaft is increased, the sliders of the VI_F travel radially outward direction or vice versa due to the centrifugal force against the friction force and the spring force, and hence develop a variable inertia into the system. Also, the speed of the sliders is controlled by two helical springs, which are connected to it.

Generally, when a fixed inertia-based diesel engine is operated under a fluctuating load, its speed is varied according to the load, and a significant speed variation is observed in the engine shaft. When the fixed inertia of the diesel engine is modified to variable inertia, the shock due to the sudden speed change of the diesel engine is adjusted initially by varying inertia, and thereafter, the fuel supply to the diesel engine is controlled using a governor. The study incorporated a VI_F into a diesel engine and operated under a variable load. The fuel supply of the engine is controlled using the PID controller by operating the throttle valve of the diesel engine.

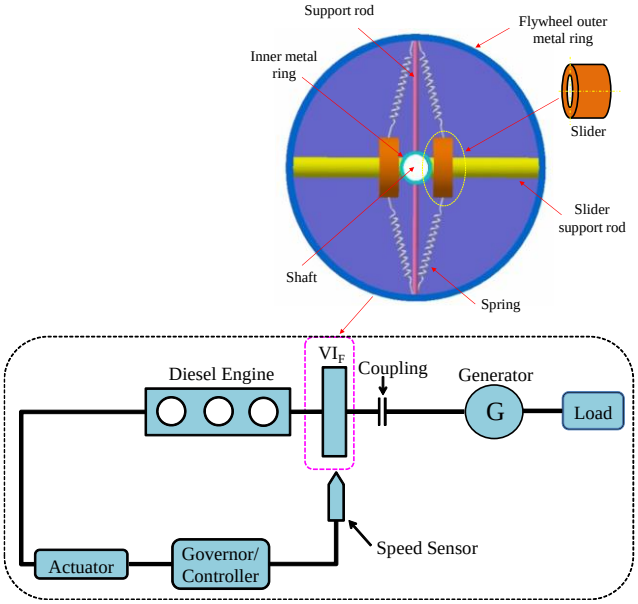

Fig. 1 Schematic diagram of a diesel engine with VI_F

2.1. Bond graph technique

The BG modelling technique has been briefly described in this section to improve the readability of the work to those who are less familiar with such technique. In the BG, the components of the system are joined by lines known as power bonds. It carries information of the effort and flow. The power variables of different energy domains are given in Table 1.

Table 1
Variables of power in different energy forms

Variables of power		
Systems	Effort	Flow
Hydraulic	Pressure	Volume flow rate
Mechanical	Force	Velocity
Mechanical	Torque	Angular velocity
Electrical	Voltage	Current
Thermal	Temperature	Entropy change rate

The power bonds together with the lumped elements, represented by letter codes, evolve into BG model of the system. In BG, the basic elements are C, I, R, SE, SF, TF, GY and junction elements 0 and 1.

2.1.1. The compliant element (C)

It functions as an energy storage element of the systems just like an electrical capacitor or a spring. The general constitutive relation for a compliant element is expressed as:

$$e(t) = K \int_{-\infty}^{t} f(\xi) d\xi \,. \tag{1}$$

The term $f(\xi)$ represents the flow which gets related to the effort $e(t)$ through the compliant element.

2.1.2. The inertial element (I)

This element represents inertia effect and establishes a relation between applied effort $e(\xi)$ and flow $f(t)$ as

$$f(t) = \frac{1}{m} \int_{-\infty}^{t} e(\xi) d\xi \,. \tag{2}$$

2.1.3. The resistive element (R)

For this element, effort to flow and flow to effort are directly related unlike inertial or compliance element (R) which relates integration of effort or flow to flow and effort, respectively.

$$e = \varphi(f) \,, \tag{3}$$

$$f = \psi(e) \,, \tag{4}$$

where φ and ψ are the functions of flow and effort respectively.

2.1.4. The source of effort (SE) and source of flow (SF)

The SE element determines the effort variable in its associated bond, however, unlike C, I and R elements, the effort is not influenced by flow. The SF element determines the flow variable in its associated bond and its output doesn't get influenced by the effort.

2.1.5. The TF element (TF) and gyrator element (GY)

The TF element is a two-port element that means two bonds are attached to it. It functions as a mechanical lever or an electrical TF which conserves power, and scales the effort to effort, and flow to flow according to its modulus. A mechanical TF and its BG representation is shown in Fig. 2. The term $\mu = (b/a)$ denotes modulus of the TF. The flow relation is $f_2 = \mu f_1$ and effort relation is $e_1 = \mu e_2$.

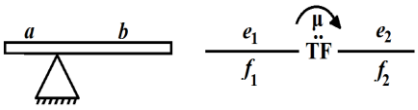

Fig. 2 TF element of BG

The only difference in the gyrator GY and TF is that unlike TF, the gyrator relates effort to flow, and flow to effort. The power remains conserved across both the element. A gyrator and its BG representation is shown in Fig. 3. The flow relation is $e_2 = \mu f_1$ and effort relation is $e_1 = \mu f_2$.

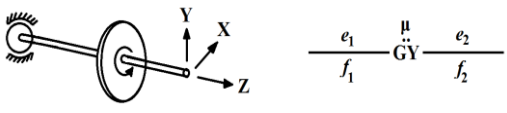

Fig. 3 Gyrator element of BG

2.1.6. The junction elements 1 and 0

There are two junction elements 1 and 0, which do not represent physical elements. Net power across them remains conserved. The 1 and 0 junctions are flow and effort equalizing junction, respectively. Assuming power direction (the half arrow on the bond represents the assigned power direction) toward junction as positive, the constitutive law for power conservation, for each junction as shown in Fig. 4 is.

$$e_1 f_1 + e_2 f_2 + e_3 f_3 + e_4 f_4 = 0 \,. \tag{5}$$

For 1 junction, where flow remains same at each of its bond, the Eq. (5) becomes.

$$e_1 + e_2 + e_3 + e_4 = 0 \,. \tag{6}$$

Similarly, for 0 junction that equalizing the effort and the Eq. (5) becomes

$$f_1 + f_2 + f_3 + f_4 = 0 \,. \tag{7}$$

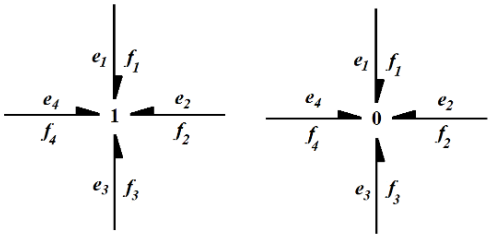

Fig. 4 Junction elements 1 and 0

2.2. Causality

In the BG, a bond exchanges both the information of effort and flow between its two ends. At the one end, an element provides either effort or flow information. The information of the other factor of the power is imparted from the opposite end. Thus, on each bond, the direction of any one factor of power has to be indicated. If one of them is indicated, then the other flows in the opposite direction. For this purpose, the convention is to put a stroke at the bond end at which the flow information is provided. In Fig. 5, a, junction 1 provides the information of flow and receives the information of effort from the 0 junction. In Fig. 5, b, junction 1 receives the information of flow and provides the information of effort to the 0 junction.

a b

Fig. 5 Information exchange in bonds: a – flow exchange, b – effort exchange

2.3. Bond graph model of the proposed diesel engine with variable inertia flywheel

The flywheel contains two sliders and four helical springs to develop the variable inertia. The sliders move outward or inward directions when the flywheel starts rotation at increasing and decreasing speeds, respectively. The bond graph model of the proposed VI_F with a diesel engine is shown in Fig. 6.

From the bond graph model of the diesel engine with VI_F (Fig. 6), a torque (T_{DE}) that developed by the diesel engine is used to operate the external load and is represented by a source of element (Se_1). In $1_{\dot{\theta}}$ junction, the resistive element ($R_3 = C_F$) represents the viscous friction resistance between the rotating shaft and the VI_F, whereas the inertial element (I_4) represents the accumulate moment of inertia of the diesel engine and the fixed mass of VI_F ($J_{DE} + J_{fxd}$). The angular speed of the diesel engine (ω_f) is detected by a source of flow element (Df_2) at the same junction. The instantaneous position of a slider can be represented by the polar coordinate system i.e., $x = r_1 cos\theta$ and $y = r_1 sin\theta$; and another slider is $x = r_2 cos(180+\theta)$ and $y = r_2 sin(180+\theta)$. The transfer functions (TF) at $1_{\dot{\theta}}$ junction convert the angular speed into linear mechanical system. The preload of the springs F_{s1} and F_{s2} are represented by source of effort elements i.e., Se_{17} and Se_{38} at $1_{\dot{r}1}$ and $1_{\dot{r}2}$ junctions, respectively. The linear displacements of both sliders are measured at the same junctions by flow detectors i.e. Df_{13} and Df_{35}. The resistive elements R_{16} and R_{40} represent the sliding frictional resistance (R_{sfrtn}) between sliders and the supporting rod of the VI_F. The padding resistance (R_{pad}) and padding stiffness (K_{pad}) is represented by resistive element R and capacitive element C, respectively. The mass of the slider (m_s) is represented by I_{12} and I_{27} elements. A variable load torque (T_{load}) is applied at $1_{\dot{\theta}}$ junction through 0 junction by a Se_{48} element.

The governing equations of the system that are obtained from the bond graph model are as follows.

$$\dot{\omega}_f = \frac{1}{\left(m_s r_1^2 + m_s r_2^2 + J_{DE} + J_{fxd}\right)} \times \times \left[T_{DE} - T_{load} - C_F \omega_f - 2m_s \left(r_1 \dot{r}_1 + r_2 \dot{r}_2\right) \omega_f\right], \quad (8)$$

$$2k_s \left[\sqrt{\left(R_i^2 + r^2\right)} - \sqrt{\left\{R_i^2 + \left(r_{iro} + 0.5 l_s\right)^2\right\}}\right] \times \times sin\alpha - R_{sfrtn} \dot{r}_1 - m_s \ddot{r}_1 - m_s \omega_f^2 r_1 = 0, \quad (9)$$

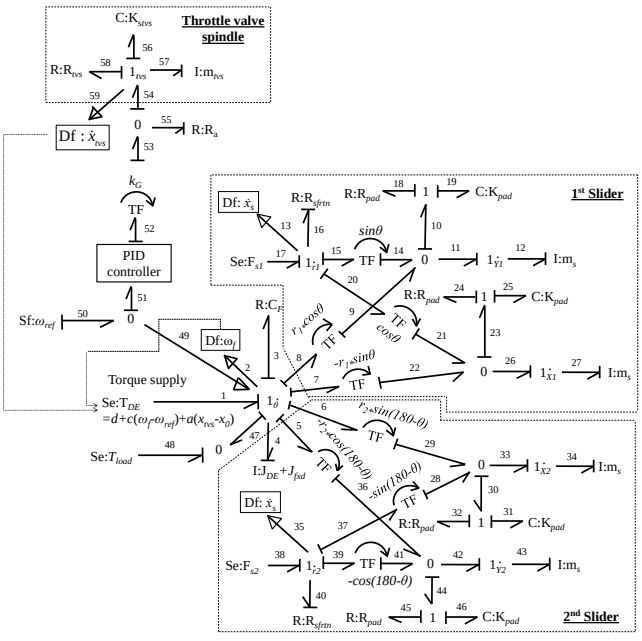

Fig. 6 Bond graph model of the diesel engine with VI_F

$$2k_s \left[\sqrt{\left(R_i^2 + r^2\right)} - \sqrt{\left\{R_i^2 + \left(r_{iro} + 0.5 l_s\right)^2\right\}}\right] \times \times sin\alpha - R_{sfrtn} \dot{r}_2 - m_s \ddot{r}_2 - m_s \omega_f^2 r_2 = 0, \quad (10)$$

$$\ddot{x} = \frac{1}{m_{tvs}} \left[k_G u R_a - R_{tvs} \dot{x}_{tvs} - K_{stvs} x_{tvs}\right]. \quad (11)$$

From Eq. (8), the angular speed of the flywheel is estimated, and it is obtained from the junction $1_{\dot{\theta}}$. It also represents the dynamical characteristic equation of the diesel generator. As per [17-19], the diesel engine torque T_{DE} is varied in a linear fashion and it depends on the fuel throttle valve spindle position (x_{tvs}) and rotational speed (ω_f). Therefore, it can be written as $T_{DE} = f(x_{tvs}, \omega_f)$. The linear expression of the T_{DE} around the rated speed is given in [19], and it is expressed as:

$$T_{DE} = d - c\Delta\omega - a\Delta x \quad (12)$$

where d, c and a are the engine torque coefficients; $\Delta\omega = (\omega_{ref} - \omega_f)$ and $\Delta x = (x_0 - x_{tvs})$. The ω_{ref} and x_0 are the rated speed of the flywheel and rated displacement of the fuel throttle valve spindle displacement, respectively.

The Eq. (9) and Eq. (10) are estimated from $1_{\dot{r}1}$ and $1_{\dot{r}2}$ junctions. These Eqs. are used for obtaining the instantaneous position or the travel length of the sliders. The free-body diagram of the slider of the flywheel is shown in Fig. 7. In the diagram, the slider's outward travel movement is shown. However, the friction force and the inertia force directions may change during the inward travel of the slider. In Eq. (9) and Eq. (10), the first term is the spring force (F_s), the second term is the frictional force (F_f), the third term is the inertia force (F_i), and the fourth term is the centrifugal force (F_c) makes the equilibrium to the slider movement. The Eq. (11) is utilized to obtain the displacement of the throttle valve spindle (x_{tvs}).

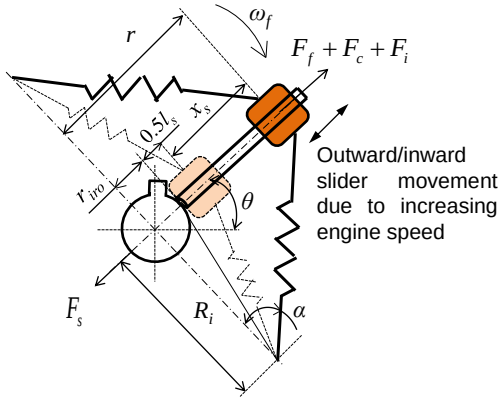

Fig. 7 Free body diagram of the slider

2.2. Inertia estimation of the VI_F

To calculate the total moment of inertia of the flywheel (J_{vif}), it is divided into two parts such as fixed parts and variable parts. In the proposed flywheel, the inertia is varied due to the movement of the sliders. The inertia of the fixed part of the flywheel (J_{fxd}) includes the sum of the individual inertia of all the components like outer ring, main rod, support rod, inner ring, cover and springs whereas the

variable inertia is produced due to the slider's movement. Therefore, the cumulative moment of inertia of the diesel engine with variable inertia flywheel (J_T) is expressed as:

$$J_T = J_{DE} + J_{vif}\,, \tag{13}$$

$$J_{vif} = J_{fxd} + nJ_s\,, \tag{14}$$

$$J_{fxd} = J_{oring} + 2J_{mr} + 4J_{sr} + J_{iring} + 2J_{fc}\,. \tag{15}$$

From Eqs. (13-15), the J_{DE} is the inertia of the diesel engine; J_s and n are inertia of the slider and number of sliders in the VI_F. The J_{oring}, J_{mr}, J_{sr}, J_{iring} and J_{sr} are the inertia of the outer ring, main rod, support rod, inner ring and face cover, respectively. The J_s is variable, and it depends on the slider movement. So, it is expressed as:

$$J_s = \frac{1}{12} m_s \left\{ \frac{3}{4}\left({d_{so}}^2 + {d_{si}}^2 \right) + {l_s}^2 \right\} + m_s r^2 \tag{16}$$

where d_{so}, d_{si} and l_s are the outer diameter, inner diameter and length of the sliders, respectively. The inertia of the outer ring J_{oring}, main rod J_{mr}, support rod J_{sr} and J_{iring} are calculated from Eqs. (17-20), respectively:

$$J_{oring} = 0.5 m_{or} \left({R_{oro}}^2 + {R_{ori}}^2 \right), \tag{17}$$

$$J_{mr} = \frac{1}{4} m_{mr} \left(\frac{{d_{mr}}^2}{4} + \frac{{l_{mr}}^2}{3} \right), \tag{18}$$

$$J_{sr} = \frac{1}{4} m_{sr} \left(\frac{{d_{sr}}^2}{4} + \frac{{l_{sr}}^2}{3} \right), \tag{19}$$

$$J_{iring} = 0.5 m_{ir} \left({r_{iro}}^2 + {r_{iri}}^2 \right), \tag{20}$$

where m_{or}, m_{mr}, m_{sr} and m_{ir} are the mass of the outer ring, main rod, support rod and inner ring, respectively. The R_{oro} and R_{ori} are the outer and inner radius of the outer ring, respectively; d_{mr} and l_{mr} are the diameter and the length of the main rod, respectively; d_{sr} and l_{sr} are the diameter and the length of the support rod, respectively; r_{iro} and r_{iri} are the outer and inner radius of the inner ring, respectively.

2.3. Modeling of the PID controller to control the throttle valve spindle position

When the load of the diesel engine is suddenly changed, the speed of the flywheel is changed accordingly until the fuel supply to the engine is not adjusted. The fuel supply of the diesel engine is controlled by adjusting the displacement of the throttle valve spindle, and the same is controlled by a suitable controller i.e. PID controller [27]. The PID control scheme of the diesel engine with VI_F is shown in Fig. 8.

3. Results and Discussion

The simulation parameters and its value are shown in Table 2.

The torque development by the diesel engine is varied according to the sudden change of the load and hence the speed of the flywheel is varied. The stability of the flywheel speed due to sudden load change is restored as quickly as by adjusting the fuel supply to the diesel engine. The fuel supply adjustment is performed by the PID controller by controlling the displacement of the throttle valve spindle. It compares the instantaneous speed of the flywheel with the reference speed, and sends a signal to the actuator, which takes the action to open or close the throttle valve. As this study develops the variable inertia, so it reduces the transition time period of the flywheel speed variations and hence improves the fuel supply of the diesel engine. From Fig. 9, a, it is representing the load torque change to the diesel engine. Initially, for first 3 s the engine is operated under zero load. Subsequently, it is operated under 280 Nm for 3-6 s, 70 Nm for 6-9 s, 280 Nm for 9-12 s, 70 Nm for 12-15 s

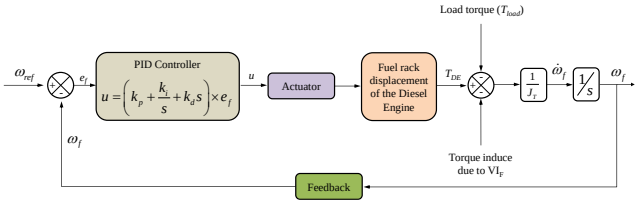

Fig. 8 Block diagram of the PID controller scheme to control the throttle valve spindle displacement

Table 2

Simulation parameters

Parameters	Value	Units
Flywheel radius or outer radius of outer ring (R_{oro})	0.2	m
Inner radius of outer ring (R_{ori})	0.19	m
Thickness of the flywheel	0.1	m
Outer radius of the inner ring (r_{iro})	0.02	m
Inner radius of inner ring, (r_{iri})	0.015	m
Slider length (l_s)	0.03	m
Outer diameter of the slider (d_{so})	0.09	m
Inner diameter of the slider (d_{si})	0.03	m
Diameter of the main rod (d_{mr})	0.03	m
Length of the main rod (l_{mr})	0.165	m
Diameter of support rod (d_{sr})	0.005	m
Length of the support rod (l_{sr})	0.165	m
Stiffness of the spring (k_s)	57996	N/m
Sliding friction resistance between slider and the supporting rod of the VI_F (R_{sfrtn})	323	Ns/m
Viscous damping resistance of the diesel engine with VI_F (C_F)	0.097	Nms/rad
Inertia of the diesel engine (J_{DE})	71.8	kgm^2
Coefficient of engine torque (d)	15.042	
Coefficient of engine torque (c)	2.095	
Coefficient of engine torque (a)	1245	
Rated speed of the flywheel (ω_{ref})	150	rad/s
Rated displacement of the throttle valve (x_0)	5×10^{-3}	m
Load torque (T_{load})	280	Nm
Gain of speed actuator (k_G)	0.15	
Delay time	2	ms
Throttle valve spindle's Resistance (R_{tvs})	10.22	Ns/m
Stiffness of the throttle valve spindle (K_{stvs})	344	N/m
Mass of the throttle valve spindle (m_{tvs})	0.5	kg
Line resistance (R_a)	1	Ns/rad
Proportional gain	0.8	
Integral gain	0.001	
Derivative gain	0.2	

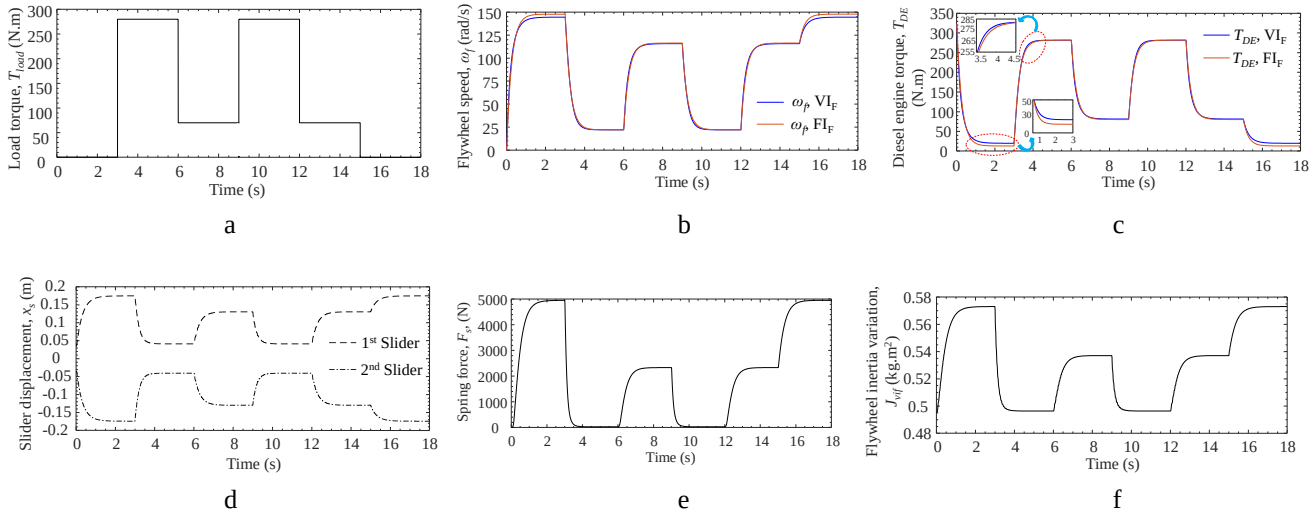

Fig. 9 Engine load and comparative results: a – load torque T_{load}, b – comparison of ω_f between VI$_F$ based diesel engine and FI$_F$ based diesel engine, c – comparison of T_{DE} between VI$_F$ based diesel engine and FI$_F$ based diesel engine, d – slider's displacement, e – spring force F_s, f – flywheel inertia variation J_{vif}

and again, zero load for 15-18 s. The diesel engine is operated on the stated load by incorporating a VI$_F$ and a FI$_F$, separately. The inertia of the FI$_F$ is considered to be the same as the maximum inertia of the VI$_F$. Comparative results are presented in Fig. 9, b and Fig. 9, c, when VI$_F$ and FI$_F$ are incorporated in the diesel engine and T_{load} is varied. Fig. 9, b shows the speed of the VI$_F$ (ω_f), whereas Fig. 9, c represents the T_{DE}, respectively. From Fig. 9, b, it is found that at zero load condition (0-3 s), the ω_f of the VI$_F$ - based diesel engine is 144 rad/s, whereas for the FI$_F$ - based diesel engine, the ω_f is 148 rad/s. For next subsequent time period (3-18 s), when load is varied, it is observed that the speed variation is reduced in VI$_F$ - based diesel engine. Therefore, the incorporation of the VI$_F$ instead of the FI$_F$ in the diesel engine, the speed variation is reduced. Similarly, from Fig. 9, c, the torque development T_{DE} from the diesel engine is higher when the VI$_F$ is incorporated instead of the FI$_F$ during no load condition, and at loading condition, the T_{DE} is slightly higher. Therefore, the torque requirement to operate the load is lower when VI$_F$ is incorporated instead of the FI$_F$ into the diesel engine.

In VI$_F$ - based diesel engine, as the ω_f is changed with the variation of T_{load}, the flywheel slider displacement x_s or the radius of rotation of the slider (r) is also varied (Fig. 9, d). The x_s is 0.17 m when flywheel rotates with high speed (almost 144 rad/s) and x_s is 0.04 m when flywheel rotates with low speed (23 rad/s). Further, the x_s value is changed according to the variation of the ω_f. The proposed design of the flywheel contains two sliders and these are travelled in opposite directions to each other. Therefore, the 1st sliderdisplacement is shown in positive, whereas the 2nd slider is shown in negative with same value. In VI$_F$, the slider is hold by two springs. The spring force in each spring is plotted in Fig. 9, e. The spring force is varied from 0 - 4930 N.

The sudden change of the T_{load} in the VI$_F$ - based diesel engine may be realized in the form of the sudden change of the flywheel speed. When T_{load} is increased or decreased, the ω_f is decreased or increased suddenly. The inertia of the VI$_F$ helps to stabilize the ω_f before fuel supply amount is not increased or decreased. The effect of load torque change can be minimized by varying the inertia of the flywheel and controlling the operation of the fuel throttle valve spindle displacement. The proposed scheme of the VI$_F$ is capable of varying the inertia, and it is estimated from Eq. (13), where it is depended on the inertia of the slider J_s. The J_s depends on the radius of rotation of the slider or displacement of the sliders. The inertia of the flywheel J_{vif} is plotted in Fig. 9, f. The J_{vif} is varied from 0.48 kgm^2 to 0.57 kgm^2.

4. Parameter Influences on the Performance

The parameters which influence the system performance are discussed in the section. In this regard, the parameters i.e. C_F, k_s, and R_{sfrtn} are identified and their influence are discussed.

4.1. Effect of the viscous friction resistance (C_F)

To analyze the influence of the C_F, its value has been varied to 0.01 - 0.3 and system responses are plotted in Fig. 10. From Fig. 10, a, it is found that with increasing the C_F value the speed of the VI$_F$ is decreased whereas the diesel engine torque T_{DE} is increased, and it is reported in Fig. 10, b. Similarly, the slider displacement (x_s) is decreased with increase of the C_F (Fig. 10, c). The VI$_F$ inertia generation depends on the slider displacement. Therefore, the VI$_F$ inertia variation is also decreased with increase of the C_F (Fig. 10, d). Note: only one slider displacement is shown here. The second slider displacement is same, but direction is opposite.

4.2. Effect of the spring stiffness of the VI$_F$ (k_s)

To analyze the influence of the k_s, its value has been varied to 50000 – 62000 N/m and system responses are plotted in Fig. 11. The k_s is the internal parameter of the spring of the VI$_F$. Therefore, with the variation of the k_s, the ω_f and T_{DE} are not changed (Fig. 11, a and 11, b, respectively). However, the x_s and J_{vif} are varied with the change of the k_s of the spring. From Fig. 11, c and 11, d, it is found

that with the increase of the k_s value, the x_s and J_{vif} of the VI$_F$ both are decreased.

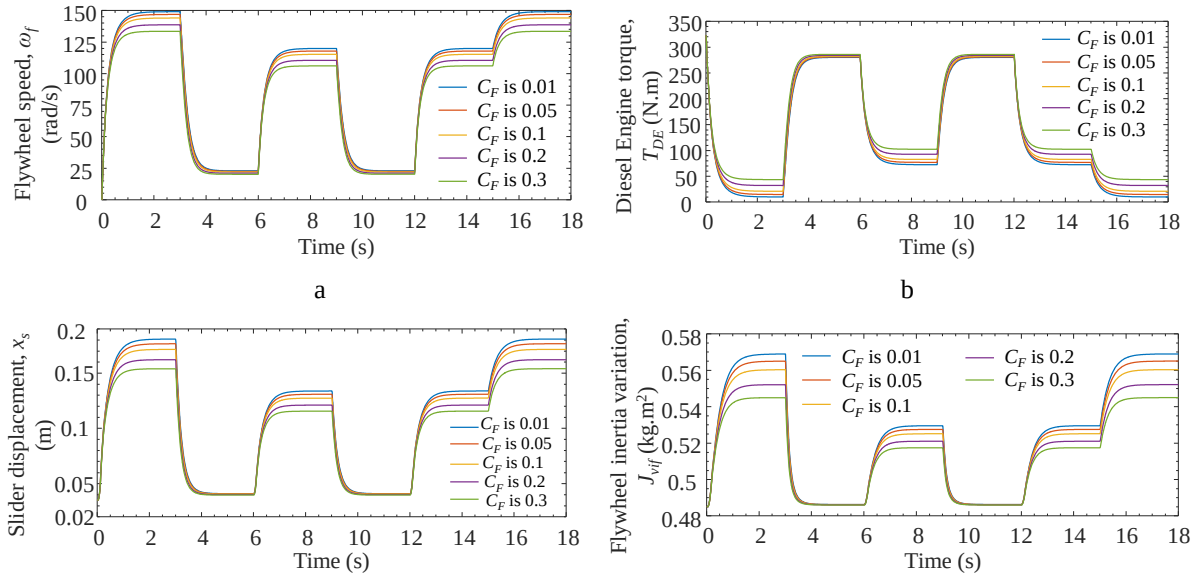

Fig. 10 Influence of C_F: a – VI$_F$ speed ω_f, b – T_{DE}, c - slider displacement x_s, d – VI$_F$ inertia J_{vif}

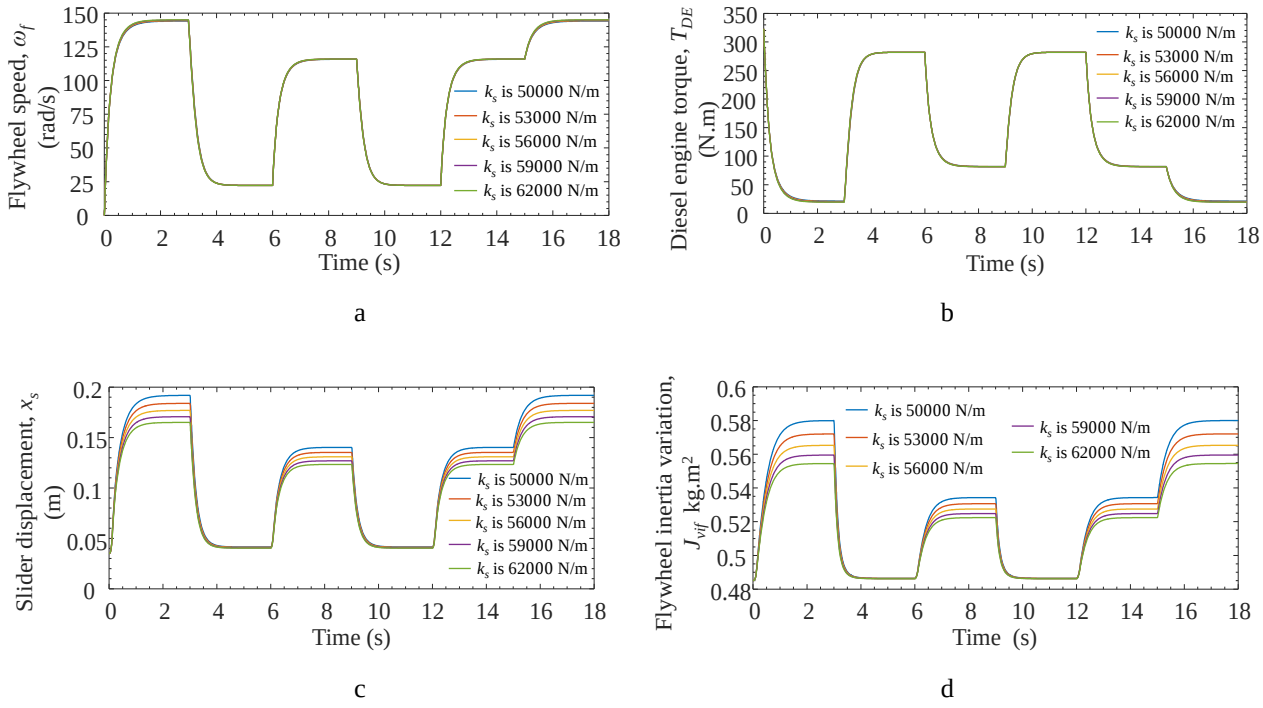

Fig. 11 Influence of k_s: a – VI$_F$ speed ω_f, b – T_{DE}, c - slider displacement x_s, d – VI$_F$ inertia J_{vif}

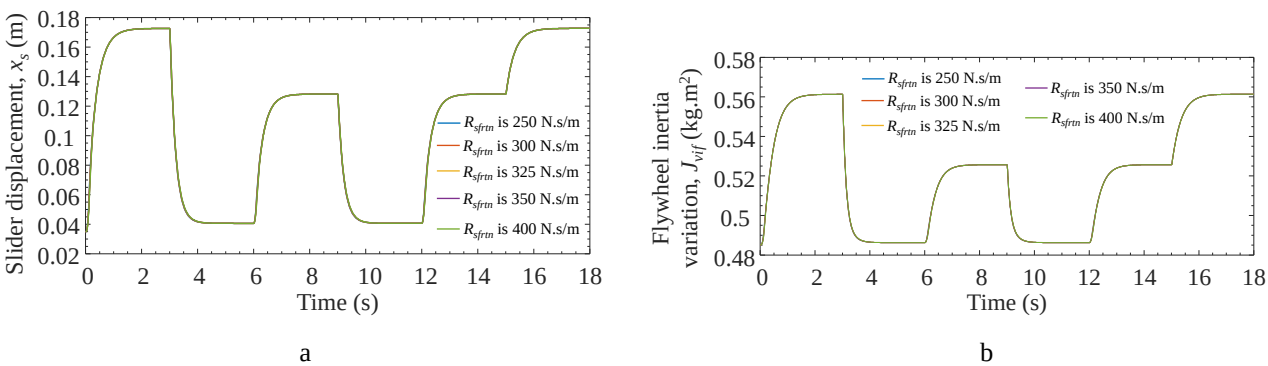

Fig. 12 Influence of R$_{sfrtn}$: a – slider displacement x_s, b – VI$_F$ inertia J_{vif}

4.3. Effect of the sliding friction resistance (R_{sfrtn})

The impact of the sliding friction (R_{sfrtn}) on the system performance is shown in Fig. 12, a, and Fig. 12, b. It is found that with the variation of the R_{sfrtn}, the slider displacement and inertia variation the VI_F are almost negligible. The other responses i.e. ω_f and T_{DE} are also unalterable with variation of R_{sfrtn}. Therefore, it is not require to be shown here.

4. Conclusions

The work proposes a new scheme based on the spring-slider mass displacement to obtain variable inertia that can effectively be utilized in diesel engines as a flywheel to reduce the shock upon the change of sudden load. The proposed VI_F provides auto inertia adjustment capability before controlling the fuel supply to the diesel engine, and hence it reduces the speed fluctuation and vibration of the system. Also, the proposed VI_F can reduce the starting torque of the diesel engine as its weight is lighter as compared to the conventional fixed inertia-based flywheel. The findings that are concluded from the study are as follows.

- The conventional fixed inertia-based flywheel can be replaced by a VI_F.
- The dynamic model of the diesel engine with VI_F is modelled using bond graph technique and simulated in SYMBOL SHAKTI software.
- The inertia of the proposed VI_F can be varied from 0.48 kg/m^4 to 0.58 kg/m^4 when the torque load is varied from 0 – 250 Nm.
- It is found that the viscous friction resistance (C_F) and spring stiffness of the VI_F (k_s) effect the system performance significantly. However, another parameter i.e. sliding friction resistance (R_{sfrtn}) does not effect the system performance so far.

The performance of the proposed scheme of the VI_F can be experimentally validated in future work. Also, the parameters of VI_F can be optimized and the control stability of the system can be verified.

Competing interests: The authors declare that they have no known competing financial interests or personal relationships that could have appeared to influence the work reported in this paper.

Financial support: The authors declare that the study has not been funded by any organization.

References

1. **Genta, G.** 1985. Kinetic Energy Storage: Theory and Practice of Advanced Flywheel Systems. London: Butterworth Heinemann Ltd. 362p.
2. **Yang, Y.; Chen, P.; Liu, Q.** 2021. A wave energy harvester based on coaxial mechanical motion rectifier and variable inertia flywheel, Applied Energy 302; 117528. https://doi.org/10.1016/j.apenergy.2021.117528.
3. **Dong, X.; Xi, J.; Chen, P.; Li, W.** 2018. Magneto-rheological variable inertia flywheel, Smart Materials and Structures 27(11): 115015. https://doi.org/10.1088/1361-665X/aad42b.
4. **Jia, Y., H.; Xu, S., J.** 2008. Spacecraft adaptive attitude control using variable inertia wheels, Journal of Astronautics 29(3):838-843.
5. **Kumar, D.; Mahato, A. C.** 2023. Various concepts on variable inertia flywheel in rotating system, in: Maurya, A., Srivastava, A.K., Jha, P.K., Pandey, S.M. (eds) Recent Trends in Mechanical Engineering. Lecture Notes in Mechanical Engineering: 527-536. https://doi.org/10.1007/978-981-19-7709-1_53.
6. **Van de Ven, J.** 2009. Fluidic variable inertia flywheel, in 7th International Energy Conversion Engineering Conference: 2-5th August 2009, Denver, Colorado. https://doi.org/10.2514/6.2009-4501.
7. **Jauch, C.; Hippel, S.** 2016. Hydraulic–pneumatic flywheel system in a wind turbine rotor for inertia control, IET Renewable Power Generation 10(1): 33-41. https://doi.org/10.1049/iet-rpg.2015.0223.
8. **Braid, J.** 2014. Conceptual design of a liquid-based variable inertia flywheel for microgrid applications, 2014 IEEE International Energy Conference (ENERGYCON): 1291-1296. https://doi.org/10.1109/ENERGYCON.2014.6850589.
9. **Burstall, O. W.** 2005. Variable inertia flywheel, Perkins Engines Co Ltd, U.S. Patent US6883399B2.
10. **Wagner, J. T.** 1992. Energy storage flywheels using fluid transfer to vary moments of inertia, U.S. Patent US5086664A.
11. **Lewis, O. G.** 1966. Variable inertia liquid flywheel, ExxonMobil Research and Engineering Co, U.S. Patent US3248967.
12. **Harrowell, R. V.** 1994. Elastomer flywheel energy store, International Journal of Mechanical Sciences 36(2): 95-103. https://doi.org/10.1016/0020-7403(94)90078-7.
13. **Li, C.; Liang, M.** 2012. Characterization and modeling of a novel electro-hydraulic variable two-terminal mass device, Smart Materials and Structures 21(2): 025004. https://doi.org/10.1088/0964-1726/21/2/025004.
14. **Xu, T.; Liang, M.; Li, C.; Yang, S.** 2015. Design and analysis of a shock absorber with variable moment of inertia for passive vehicle suspensions, Journal of Sound and Vibration 355: 66-85. https://doi.org/10.1016/j.jsv.2015.05.035.
15. **Yang, S.; Xu, T.; Li, C.; Liang, M.; Baddour, N.** 2016. Design, modeling and testing of a two-terminal mass device with a variable inertia flywheel, ASME Journal of Mechanical Design 138(9): 095001. https://doi.org/10.1115/1.4034174.
16. **Ning, D.; Sun, S.; Yu, J.; Zheng, M.; Du, H.; Zhang, N.; Li W.** 2019. A rotary variable admittance device and its application in vehicle seat suspension vibration control, Journal of the Franklin Institute 356(14): 7873-7895. https://doi.org/10.1016/j.jfranklin.2019.04.015.
17. **Yuan, L. G.; Zeng, F. M.; Xing, G. X.** 2010. Research on the design and control strategy of variable inertia flywheel in diesel generator unit under pulsed load, International Conference on Computing, Control and Industrial Engineering, 5-6th June 2010, Wuhan, China. https://doi.org/10.1109/CCIE.2010.55.
18. **Li, T.; Zeng, F.; Qin, J.** 2011. The determination of rotational inertia of flywheel for pulsed-load diesel Gener-

ator, Second International Conference on Mechanic Automation and Control Engineering, 15-17th July 2011, Inner Mongolia, China. https://doi.org/10.1109/MACE.2011.5987054.
19. **Zhang, Y.; Zhang, X.; Qian, T.; Hu, R.** 2020. Modeling and simulation of a passive variable inertia flywheel for diesel generator, Energy Reports 6: 58-68. https://doi.org/10.1016/j.egyr.2020.01.001.
20. **Mahato, A. C.; Ghoshal, S. K.; Samantaray, A. K.** 2019. Influence of variable inertia flywheel and soft switching on a power hydraulic system, SN Applied Sciences 1: 605. https://doi.org/10.1007/s42452-019-0623-0.
21. **Kushwaha, P.; Ghoshal, S. K.; Dasgupta, K.** 2020. Dynamic analysis of a hydraulic motor drive with variable inertia flywheel, Proceedings of the Institution of Mechanical Engineers, Part I: Journal of Systems and Control Engineering 234(6): 734-747. https://doi.org/10.1177/0959651819875914.
22. **Li, Q.; Li, X.; Mi, J.; Jiang, B.; Chen, S.; Zuo, L.** 2020. A tunable wave energy converter using variable inertia flywheel, IEEE Transactions on Sustainable Energy 12(2): 1265-1274. https://doi.org/10.1109/TSTE.2020.3041664.
23. **Yamamoto, T.; Kondoh, J.** 2020. Development of a self-inertia-varying fixed-speed flywheel energy storage system, In 23rd International Conference on Electrical Machines and Systems (ICEMS-2020), 24-27rd November 2020, Hamamatsu, Japan. https://doi.org/10.23919/ICEMS50442.2020.9291150.
24. **Mukherjee, A.; Karmakar, R.; Samantaray, A. K.** 2006. Bond graph in modeling, simulation and fault identification, 2nd edition. New Delhi: CRC Press. 244p.
25. **Emami, M. D.; Mostafavi, S. A.; Asadollahzadeh, P.** 2011. Modeling and simulation of active hydro-pneumatic suspension system through bond graph, Mechanika 17(3): 312-317. https://doi.org/10.5755/j01.mech.17.3.509.
26. **Samantaray, A. K.; Mukherjee, A.** 2006. User's Manual of SYMBOLS Shakti, High-Tech Consultants STEP, Indian Institute of Technology Kharagpur.
27. **Senthilkumar, P.; Sivakumar, K.; Kanagarajan, R.; Kuberan, S.** 2018. Fuzzy Control of Active Suspension System using Full Car Model, Mechanika 24(2): 240-247. https://doi.org/10.5755/j01.mech.24.2.17457.

P. R. Mahto, A. C. Mahato

DYNAMIC MODELLING AND ANALYSIS OF A NEW DESIGN VARIABLE INERTIA FLY-WHEEL FOR DIESEL ENGINE USING BOND GRAPH TECHNIQUE

S u m m a r y

The work proposed a new methodology to obtain variable inertia that reduces the speed fluctuations of the diesel engine during sudden load variations in terms of a variable inertia flywheel (VI_F). In the proposed VI_F, the inertia variation technique is based on the slider mass movement supported by the springs. The sliders of the VI_F travel outward or inward according to the speed increase or decrease of the diesel engine, and hence, it produces variable inertia. It helps to reduce sudden speed fluctuations by adjusting the inertia before adjusting the fuel supply to the diesel engine. A dynamic model of the VI_F with a diesel engine is developed using the bond graph technique and simulated in SYMBOLS SHAKTI software. Moreover, the simulation responses of the VI_F with a diesel engine are compared with the same diesel engine when a fixed inertia flywheel (FI_F) is attached to it. The simulation results show that the inertia of the flywheel can be varied from 0.48 kg/m^4 to 0.57 kg/m^2, and speed fluctuations of the diesel engine can be reduced when a VI_F is attached to it instead of a FI_F. Moreover, it is found that the viscous friction resistance (C_F) and spring stiffness of the VI_F (k_s) effect the system performance significantly and another parameter i.e. sliding friction resistance (R_{sfrtn}) does not effect the system performance.

Keywords: variable inertia, diesel engine, dynamical system modeling, PID controller, bond graph.

Received December 26, 2023
Accepted December 16, 2024